Genuinely ferroelectric sub-1-volt-switchable nanodomains in HfxZr(1-x)O2 ultrathin capacitors

Journal:	*ACS Applied Materials & Interfaces*
Manuscript ID	am-2018-07988n.R2
Manuscript Type:	Article
Date Submitted by the Author:	n/a
Complete List of Authors:	Stolichnov, Igor; EPFL-EPFL-Swiss Federal Institute of Technology Cavalieri, Matteo; EPFL-EPFL-Swiss Federal Institute of Technology Colla, Enrico; EPFL-EPFL-Swiss Federal Institute of Technology Schenk, Tony; NaMLab gGmbH, Mittmann, Terence; NaMLab gGmbH Mikolajick, Thomas; NaMLab and TU Dresden, Schroeder, Uwe; NaMLab gGmbH Ionescu, Adrian; Ecole Polytechnique Fédérale de Lausanne, Engineering

Genuinely ferroelectric sub-1-volt-switchable nanodomains in $Hf_xZr_{(1-x)}O_2$ ultrathin capacitors

Igor Stolichnov[1], Matteo Cavalieri[1], Enrico Colla[2], Tony Schenk[3], Terence Mittmann[3], Thomas Mikolajick[4], Uwe Schroeder[3], and Adrian M. Ionescu[1]*

[1] Nanoelectronic Devices Laboratory, Ecole Polytechnique Fédérale de Lausanne (EPFL), Lausanne 1015, Switzerland

[2] Materials Departament, Ecole Polytechnique Fédérale de Lausanne (EPFL), Lausanne 1015, Switzerland

[3] Namlab gGmbH, Noethnitzer Strasse 64, 01187 Dresden, Germany

[4] *Chair of Nanoelectronic Materials, TU Dresden, 01062 Dresden, Germany*

*Corresponding author's e-mail: igor.stolitchnov@epfl.ch

Keywords: ferroelectrics, non-volatile memory, hafnium oxide, low-voltage switching, PFM spectroscopy, domain nucleation

ABSTRACT

The new class of fully silicon-compatible hafnia-based ferroelectrics with high switchable polarization, good endurance and thickness scalability shows a strong promise for new generations of logic and memory devices. Among other factors, their competitiveness depends on the power efficiency that requires reliable low-voltage operation. Here, we show genuine ferroelectric switching in $Hf_xZr_{(1-x)}O_2$ (HZO) layers in the application-relevant capacitor geometry, for driving signals as low as 800mV and coercive voltage below 500mV. Enhanced Piezoresponse Force Microscopy (PFM) with sub-picometer sensitivity allowed for probing individual polarization domains under the top electrode and performing a detailed analysis of hysteretic switching. The authentic local piezoelectric loops and domain wall movement under bias attest to the true ferroelectric nature of the detected nano-domains. The systematic analysis of local piezoresponse loop arrays reveals a totally unexpected thickness dependence of the coercive fields in HZO capacitors. The thickness decrease from 10nm to 7 nm is associated with a remarkably strong decrease of the coercive field, with about 50% of the capacitor area switched at coercive voltages ≤0.5V. Our explanation consistent with the experimental data involves a change of mechanism of nuclei-assisted switching when the thickness decreases below 10nm. The practical implication of this effect is a robust ferroelectric switching under the millivolt-range driving signal, which is not expected for the standard coercive voltage scaling law. These results demonstrate a strong potential for further aggressive thickness reduction of HZO layers for low-power electronics.

1. INTRODUCTION

Ferroelectric materials exhibiting electrically reversible spontaneous polarization offer a wealth of useful functionalities for information processing and storage. Non-volatile ferroelectric memories[1], spintronic elements[2], domain-wall-based electronics[3], steep-slope switches relying on the negative capacitance effect[4] are among the extensively studied applications, however the integration on silicon has been remaining a major issue with traditional perovskite ferroelectrics. The ground-breaking discovery of ferroelectricity in doped HfO_2[5,6] and $Hf_xZr_{(1-x)}O_2$ (HZO) thin films[7] solves the long-standing integration issue making the ferroelectrics CMOS-compatible without compromising the switching polarization and other functional properties[8]. This discovery was followed by active studies of non-volatile ferroelectric memory devices using HfO_2-based hysteretic elements, and the new materials proved to be a viable replacement of conventional ferroelectrics for ferroelectric capacitors[9] or ferroelectric field effect transistors[10]. On the other hand, the studies revealed a complex switching process characterized by a delicate balance of ferroelectric and non-ferroelectric phases[11,12], which can be influenced by the voltage cycling (wake-up procedure)[13]. It has been demonstrated that the ferroelectric phase is stable in doped HfO_2 layers with thickness of 10-12nm[14] or lower, where the prominent switching polarization is observed. This is in a stark contrast with the behavior of perovskite-type ferroelectrics, which typically exhibit a significant degradation of their switching properties for thickness below 50nm due to the depolarization effect. The excellent thickness scalability of HfO_2-based ferroelectrics is very attractive for functional electronics since, ideally, the operation voltage can be downscaled directly with the thickness. However, the studies of sub-10nm films show that the coercive voltage tends to stabilize close to 1V and its further reduction proves to be challenging. The coercive voltage below 1V has been reported by Park et al.[15] for 5.5nm HZO capacitors, however the switching polarization significantly decreased compared to the thicker samples. On the other hand, for thinnest HZO ferroelectric films of 2.5nm the coercive voltage measured using PFM was as high as 1.5-2V, and the electrostatic modelling gave the effective coercive voltage of 0.8V i.e. 3.2MV/cm[16]. This effect of anomalously high coercive field in the films with thickness below 10nm requires further in-depth analysis in view of its practical importance for low-voltage electronics.

Concurrently with the device-oriented studies there is a focus on fundamental aspects of ferroelectricity in HfO_2-based films including ab-initio simulations[17,18], structural analysis by transmission electron microscopy (TEM) and attempts to probe the polarization domains in the nanometer scale by piezoelectric force microscopy (PFM). For doped HfO_2 films the data from scanning TEM[17,19] clearly showed the existence of a non-centrosymmetric orthorhombic phase, which is compatible with ferroelectricity. It was speculated that the interfaces between the different phases can be mobile under the external bias[19], and some subtle structural variations within the non-centrosymmetric phase could be attributed to ferroelectric domains[20]. The PFM offer a technique for direct observation of polarization domains and their dynamics under electric field. The measurements performed on the bare surface of doped HfO_2 layers reveal a hysteretic electromechanical response on the nanometer scale, with the possibility to create artificial domains using the PFM probe[16,21]. Even though such results are often evoked as a proof of true ferroelectric behavior, the alternative mechanisms responsible for the hysteretic response cannot be fully excluded. In particular, PFM maps mimicking written polarization domains have been reported for non-ferroelectric films such as pure amorphous HfO2[22,23] . On such non-ferroelectric materials it was possible to measure sharp hysteresis loops with the "coercive fields" confusingly similar to the values expected from the ferroelectrics. Possible origin of such ferroelectricity-mimicking behavior can be the electrostatic forces associated with surface charging due to the injection from the tip, charged defects (i.e. oxygen vacancies) migration, electrochemical reactions on the film surface or other effects[23].

Apart from the scientific interest, discrimination between the hysteretic effects mimicking ferroelectricity and genuine ferroelectric switching is a highly application-relevant technical issue. The true ferroelectricity allows for fastest operation down to the picosecond range and brings additional usable phenomena such as the negative capacitance effect[4]. To prove genuine ferroelectricity, PFM analysis of doped HfO_2 in capacitor geometry is an essential technique, since it permits to observe the polarization domains and track their dynamics. PFM performed in the capacitor geometry allows for more reliable data interpretation compared to the bare surface[24]. The advantage of AFM measurements through the top electrode is the uniform and well-defined electric field, which is independent of the tip radius. Additionally the capacitor geometry eliminates the risk of electrochemical reactions on the film surface. For conventional ferroelectrics, there are techniques for verifying the ferroelectric origin of hysteretic response of the capacitor relying on the comparison of field-on (also called DC-on) and field-off hysteresis loops[23,25]. Recently, PFM study of domain dynamics in 10nm HZO in the capacitor geometry had been carried out[26], however, no in-depth analysis of the field-on/off loops is available so far. The absence of such an analysis for HfO_2-based hysteretic materials can be explained by experimental difficulties with accurate measurements on ≤10nm films with very weak longitudinal piezoelectric coefficient within the range of 1-10pm/V.[27, 28]

Here we demonstrate genuine ferroelectric switching in HZO, an archetypical representative of HfO_2-based hysteretic materials, in the capacitor geometry. We measure true ferroelectric domains, probe their dynamics and show that in the case of 7nm HZO capacitors switching occurs in an anomalously low bias within the millivolt range with the corresponding coercive voltage below 500mV.

2. EXPERIMENTS

For this study a series of HZO films with thickness ranging from 7 to 30 nm has been grown by atomic layer deposition (ALD) on Si/SiO_2/TiN substrate stack according to the earlier reported procedure[29]. After sputtering 12nm top TiN electrode the multilayer structure was annealed at 600°C in N_2 atmosphere. The sample preparation was completed by sputtering 20nm top layer Pt and patterning capacitors by photolithography followed by wet etching. The lateral size of the individual capacitors varied from 50x50μm^2 for the electrical characterization to 5x5μm^2 for PFM analysis. Polarization loops measured using the standard virtual ground circuitry with a commercially available AixACCT TF 2000 analyzer exhibit hysteretic behaviour as typical for the state-of-art HZO capacitors, with the remnant polarization of 18, 20 and 7 $\mu C/cm^2$ for HZO film thickness of 7, 10 and 30nm, respectively (see Supporting information for further characterization details). The highest value of remnant polarization was measured on the 10nm layer, which is in line with the reports indicating that this thickness is optimal for ferroelectric phase stabilization[29,30]. Prior to the experiments presented in this study all capacitors have been cycled with 10000 alternating polarity voltage pulses of 3V/1ms in order to stimulate the wake-up process[29] and ensure that no additional bias-driven phase transition occurs during the measurements.

In order to detect the individual polarization domains, track their dynamics and analyse polarization switching with nanometer resolution, we used the PFM technique, which has been specially adapted for HZO capacitors with extremely weak piezoresponse. The standard PFM technique commonly used for studying ferroelectrics including HfO_2-based materials[21] relies on detecting the piezoresponse near the resonance frequency of the cantilever. Different approaches such as Dual AC Resonance Tracking (DART)[31] or Band Excitation (BE)[32] are used for resonance frequency tracking during the measurements. The advantage of resonant PFM is obvious: the measured signal gains 1-2 orders of magnitude compared to the off-resonance signal, which allows for detection of weak electro-mechanical responses. Furthermore, the stronger signals allow for faster data acquisition, which is important for collection of large arrays of loops used in PFM spectroscopy. On the other hand, the tip-sample interaction near the resonance can be difficult to analyze as the results may depend on the parasitic non-local probe-sample interactions and/or resonance tracking accuracy. Such phenomena often play a minor role for conventional perovskites where the piezoresponse is strong, however for sub-10nm HfO_2 where the longitudinal piezoelectric coefficient d_{33} can be 3-5pm/V or less, the application of resonant PFM technique is more difficult. The off-resonance PFM (also known as non-resonance PFM) approach used in this study has the advantage of simplicity, more straightforward interpretation/quantification of the detected signal, and easier identification of possible artefacts (see Supporting Information for details). In this approach, like in all PFM methods, the sample is driven with an AC or AC + DC voltage. However, in non-resonant PFM the frequency can be chosen arbitrarily as long as the system's resonance frequencies and tip resonance frequency are avoided. Within the accessible frequency range (limited by the RC-constant) the PFM signal has to be mostly frequency-independent, which is an important criterion for the credibility of the measurements. The PFM signal can be calibrated for quantitative measurements easier than in resonant mode because the cantilever deflection directly measures the electromechanical response of the sample. The drawback of the technique is a relatively low amplitude of the cantilever deflection signal, which entails longer times of data acquisition and consequently very slow measurements (at least 1-2 orders of magnitude longer compared to the standard DART measurements). The data presented below show that despite these limitations the off-resonance PFM is capable of most sensitive measurements for accurate analysis of weakest piezoelectric responses.

3. RESULTS AND DISCUSSION

All the PFM measurements presented in this study have been carried out in the capacitor geometry, with the mechanical response sensed through the 35nm TiN/Pt top electrode. Typical local piezoresponse loops showing the amplitude and phase of effective longitudinal piezoelectric coefficient d_{33eff} measured on HZO capacitors with thickness of 7, 10 and 30nm are shown in Fig 1. The loops were stable, reproducible and frequency independent, as confirmed by collecting data at three frequencies of 12kHz, 92kHz and 230kHz, all of them being lower than the contact resonance frequency (see Supporting Information for details). The frequency-independence observed for both on-field and off-field loops indicates that the amplitude data represent the true piezoelectric response. Therefore, the amplitude can be converted to d_{33eff} via the calibration procedure as described in Supporting information. The highest saturation value of d_{33eff} measured for 10nm HZO reached 5.5pm/V, which is comparable with the earlier reported double-beam interferometry measurements with results ranging from 1pm/V for Y-doped HfO_2[27] to 10pm/V for thick ZrO_2.[28]

The measurements on HZO capacitors with thickness of 7nm, 10nm and 30nm have been carried out with an AC voltage of 0.3V, 0.5V and 0.8V, respectively, i.e. the AC amplitude was always kept below the coercive voltage. It is worth noting that in the case of 7nm capacitor the measured maximum d_{33eff} of 4pm/V converts to the remarkably small mechanical displacement of 1.3pm. Consequently the noise level of d_{33eff} of 0.2 pm/V extracted from the plot implies the sensitivity ≤0.1pm for the measurements at AC signal of 0.3V, which represents the ultimate sensitivity limit of these PFM measurements.

The most important evidence of true ferroelectric origin of the measured PFM data comes from the comparative analysis of the field-on/field-off d_{33eff} loops. The field-off loops in Fig.1 are characterized by saturation of d_{33eff} at high fields. In contrast to this behaviour, the field-on loops of 10nm and 30nm capacitors show a clear d_{33eff} decrease with voltage. This trend well known for $Pb(Zr_x,Ti_{1-x})O_3$ (PZT) and other perovskite materials represents a characteristic feature of ferroelectrics[25]. Such behaviour of field-on loops is governed by several competing factors that contribute to the d_{33}: spontaneous polarization P, dielectric permittivity ε, and domain contribution. Neglecting the domain contribution (in PFM experiments only one domain is normally located below the tip) one can represent d_{33} as follows:

$$d_{33} = 2\varepsilon\varepsilon_0 QP \qquad (1)$$

where Q is electrostriction coefficient and ε_0 is dielectric permittivity of vacuum. The polarization saturates when the voltage is high enough, while the dielectric permittivity has a more complex behavior. The nonlinear dielectric response of the lattice of ferroelectric materials results in a dielectric constant decrease under bias, which entails d_{33} decrease with increasing bias field. The theoretical analysis done for PZT based on Landau-Ginzburg-Devonshire theory describes this kind of field dependence of d_{33} [33] and the experimental data agree well with this description[25].

Another fingerprint of genuine ferroelectricity is a "hump" in field-on amplitude loop of 30nm HZO at sub-coercive voltage, which is marked by red circles in Fig.1a. This non-monotonic d_{33eff} behavior particularly clearly seen on the negative swing of the loop is also known from PZT and other perovskite films[25]. It originates from the singularity of the dielectric response near the coercive field, which overrides the polarization decrease in Eq.1 resulting in a measurable d_{33} maximum. This characteristic feature inherent for true ferroelectricity is very pronounced in 30nm HZO, which is likely to be closest to the phase transition and therefore have strongest non-linear dielectric response, in agreement with the Landau-Ginzburg-Devonshire theory. The same humps, but with lower relative magnitude are seen as well in 10nm HZO (Fig.1c) and to even lesser extent in 7nm HZO (Fig. 1e).

The sharp switching and low coercive voltage of the 7nm HZO capacitors implies its ability to switch under the driving voltage below 1V. Figure1(g,h) shows the loops measured at the amplitude of 800mV, with AC signal of 300mV/92kHz. The sharp loop with 180°-flipping phase, saturating d_{33eff} and low coercive voltages of 350-450mV illustrate the robust switching performance at the millivolt-range bias for the 7nm HZO capacitor.

PFM maps representing the amplitude and phase of local piezoelectric response have been collected for all capacitors at different switching stages in order to explore the behaviour of individual polarization domains. Figure 2 shows sequential maps collected on the same 1.4x1μm^2 area of the 10nm HZO capacitor fully poled with top electrode bias of -3V/1second (Fig. 2a), gradually reversed by +1.3V/1sec (Fig. 2b), +1.7V/1sec (Fig. 2c) and finally fully poled by +3V/1sec (Fig. 2d). The mixed states characterized by the polarization domains with the vertical component of polarization oriented upwards/downwards are clearly seen in the maps of partially poled states (Fig. 2b,c). The size of poled regions with strong d_{33} signal and uniform phase response is typically 50-200nm, which is much larger than the average grain size of the HZO film (about 20-30 nm). This indicates that within these regions the grain boundaries do not inhibit the domain growth. On the other hand, the polarization map in (Fig. 2b,c) implies the nucleation-limited switching kinetics with many boundaries blocking the sideways domain growth (as opposed to the Kolmogorov-Avrami kinetics often observed in conventional ferroelectrics)[25] This type of switching kinetics is consistent with the macroscopic measurements of switching polarization reported earleir[34]. The regions of secondary phase always presenting even in the highest quality HZO layers[12] are likely to be responsible for such complex domain growth pattern. The lateral resolution limits do not permit observing the non-ferroelectric phase regions in the PFM images, however the strong variation of amplitude even at the fully poled states (Fig. 2a,d) can be explained by the nonuniformity of the ferroelectric phase, e.g. different polarization orientation within different grains. It is worth noting that the top electrode topography that was very smooth (root-mean-square roughness is always within the sub-nanometer range) did not interfere with the PFM results.

The same measurements carried out on 7nm HZO (Fig. 3) reveal a similar domain structure at the intermediate switching states. Unlike the 10nm HZO, the switching process in this case is less homogeneous with a number of spots that fail to switch even at the maximum absolute DC bias of 1.8V (Fig. 3a,d). These spots in some cases show the phase opposite to what is expected according to the imposed polarization sign. This may signal the presence of non-ferroelectric regions[29], where the "wrong phase" of the piezoresponse is explained by the injected and trapped charges rather than spontaneous polarization. On the other hand, some areas of the 7nm HZO capacitor readily switch at remarkably low external bias of 0.7-0.9V/1sec. as shown in Fig. 3(b,c). This switching behavior is consistent with the millivolt-range hysteresis loops shown in Fig. 1(g,h). The big domains with a size of hundreds of nm that can be reversed by the millivolt-range bias imply the possibility to create individual devices entirely switchable by such a low voltage. However, some major processing challenges still need to be overcome in order to achieve a homogeneously switching 7nm HZO film that performs similar to the 10nm reference material.

PFM data for 30nm HZO were similar to the results in Figs 2 and 3 (see Supporting information).

For statistically representative switching data, in addition to the piezoresponse amplitude and phase maps we have systematically measured arrays of loops on all three HZO capacitors with thickness of 7, 10 and 30 nm. The loops were collected in arrays of 10x10 points covering the area of 1x1 μm^2, with the regular spacing of 100nm between the adjacent nodes of the grid. Figure 4 presents the distributions of coercive voltages extracted from the arrays of hysteresis loops. The color maps in Fig 4a-c visualize the coercive voltages for each individual point of the grid, and the black squares correspond to the points where no hysteresis loop could be measured.

In agreement with the piezoresponse scans in Fig.2, the 10nm HZO capacitor shows the most uniform switching, without any "black" regions and with narrowest coercive voltage distribution (Fig. 4b). For 7nm HZO (Fig. 4a), a broader distribution of coercive voltages and black non-switching zones covering about 15% of the analysed area are consistent with the domain images in Fig. 3 where some non-switching regions are clearly seen. In Fig. 3 some relatively large non-switching regions >30-40nm could be resolved in both amplitude and phase images, while smaller regions could be sensed indirectly because they are affecting the adjacent ferroelectric areas. The presence of such regions results in a substantial coercive field variation in 7nm capacitor compared to the 10nm reference structure. Despite the observed inhomogeneity of switching performance, the data in Fig. 4a confirm that more than 50% of the analysed spots switches at an average coercive voltages ≤500mV.

The coercive field map of 30nm HZO capacitor (Fig.4c) also includes a significant non-switchable fraction (about 15%). The analysis of loop shape (Fig. 1) implies that at the thickness of 30nm the material is close to the phase transition where the ferroelectric phase is replaced by the non-ferroelectric monoclinic phase[35], in agreement with the earlier reports[11]. Due to the composition inhomogeneity or other factors the transition to the non-ferroelectric phase may occur locally in some individual nanometer-sized zones of the 30nm HZO capacitor, which explains the non-switching spots in Fig.4c.

The average coercive fields calculated for all three capacitors from the data in Fig. 4a-c (excluding the non-switching spots) are plotted as a function of thickness in Fig. 4d. The resulting thickness dependence is strikingly different from the expectations. The first surprising feature is that the coercive fields measured on 10nm and 30nm capacitors are nearly the same ($E_c \approx 1.2$MV/cm), i.e. the coercive voltage scales linearly with thickness. Our analysis of the hysteresis loops in Fig. 1 shows that the 30nm capacitor has much lower phase transition temperature compared to the 10nm HZO (pronounced "humps" in the 30nm loop), and consequently much lower intrinsic coercive field should be expected from the thermodynamic approach[25]. The observed thickness independence of the coercive field strongly suggests its non-thermodynamic origin. In this case, the coercive field is controlled by the opposite domain nuclei in the interface-adjacent regions rather than the thermodynamic instability in the ferroelectric volume[36]. Polarization switching assisted by such nuclei of opposite domains occurs at fields lower than the thermodynamic coercive field and the thickness dependence of the switching process is different from the thermodynamic prediction.

The most remarkable feature in the Fig. 4d is the anomalously low average coercive field of the 7nm capacitor. In contrast to the stable coercive field of 10nm and 30nm HZO, in 7nm HZO the coercive field is almost two times lower, $E_c \approx 0.7$MV/cm, which corresponds to the average coercive voltage $V_c \approx 490$mV. This observation is against the common trend of conventional ferroelectrics: the coercive field generally increases with the film thickness decrease[37]. This effect is often analysed in terms of Janovec-Kay-Dunn law, which predicts $E_c \propto d^{-2/3}$, where d is the film thickness[38]. On the other hand, the recent study of thickness dependence of coercive fields of sub-10nm HZO[15] reported a significant coercive field decrease for 5.5nm layers. The explanation evoked the depolarization effect, which reduces the effective electric field seen by the ferroelectric [39, 40].

Here we summarize the reasons why this concept is unable to explain the anomalous E_c behaviour observed in the present study. The depolarizing field mechanism applies to the ferroelectrics where E_c increases with V_{max} (the maximum voltage applied to the ferroelectric). The depolarizing field reduces V_{max}, therefore the detected E_c decreases accordingly. Since the depolarizing field increases with the thickness decrease, the apparent effect of lowering E_c in thinner films can be observed. Because this effect is associated with the reduction of effective voltage applied the ferroelectric, the E_c decrease typically occurs concurrently with the degradation of the remanent polarization, as observed for 5.5nm HZO in Ref.[15] In contrast to this behavior, in our experiments the coercive field is independent on V_{max}. Figure 5a shows the local loops of d_{33} measured on the same spots with switching voltage amplitudes 0.8V and 1.8V. Both loops have the same E_c and very close values of d_{33} at V=0 , where d_{33} is proportional to the remanent polarization. Therefore the voltage of 0.8V is high enough for complete and stable switching of the probed region, and the depolarizing effects are unlikely to significantly change the measured E_c .

This, the anomalous decrease of coercive field in 7nm HZO is difficult to explain within the standard concepts of polarization reversal in ferroelectrics, unless some new switching mechanisms are involved. Here we propose a scenario that can rationalize the coercive field decrease in terms of two competing mechanisms of nuclei-assisted switching.

The proposed concept implies nucleation-limited switching kinetics, which is consistent with the data presented above as well as with previous reports[34]. The classic nucleation theory by Landauer[41] describes the competition of the bulk and surface energy contributions to the potential barrier for growth of the nucleus, with an additional electrostatic contribution due to the depolarizing effect. This basic theory predicts prohibitively high energy barriers for domain nucleation (Landauer's paradox)[42], however taking into account the role of interfaces and defects, one can obtain results consistent with the experimental data[36, 42]. Figure 5(b) schematically depicts the growing nuclei of opposite domains described by this model.

The nucleation process described within the classic model is generally thickness-independent. To understand the coercive field decrease observed for the 7nm HZO film we assume that in such thin films the geometry of domain nuclei drastically changes. According to this hypothesis the nuclei in 7nm HZO have cylindrical shape and expand from the bottom to top interface (Fig. 5c). Note that the thickness of 7nm can be comparable with the critical size of the nuclei[42], so their expansion through the entire film can be a realistic scenario. Furthermore, these nuclei can be stabilized by the charged defects and become non-volatile. The qualitative difference of the growth conditions for such cylindrical nuclei is that they do not need to overcome the depolarizing field (unlike the classic case shown in Fig. 5b). They expand laterally through sideways wall movement, which requires less energy, and therefore switching occurs at a lower coercive field. In principle this scenario involving the cylindrical nuclei can be envisaged for thicker films as well. However, the critical energy for the cylindrical nuclei increases linearly with the film thickness, which makes the classic nucleation mechanism more favourable for thicker films. Thus, within the proposed hypothesis the nucleation-limited switching for 10-30nm HZO is driven by the standard nucleation mechanism (weak thickness dependence of the coercive field), whereas for 7nm capacitors the cylindrical nuclei promote switching at a lower coercive field. Apart from the theoretical interest this change of switching mechanism implies new potential for reduction of operation voltage in ultra-thin capacitors, which opens tantalizing perspectives for applications.

4. CONCLUSIONS

In conclusion, the whole body of data from HZO capacitors presented in this study highlights a striking resemblance between the switching behaviour of HZO and conventional perovskite ferroelectrics like PZT. The authentic shape of field-on/field-off piezoelectric hysteresis loops, size, structure and field-driven evolution of polarization domains look very similar to the earlier reported data from PZT film capacitors. A number of observed characteristic features of the switching process are considered as signatures of true ferroelectricity. These features, in particular the authentic shape of the loops, are not consistent with the competing non-ferroelectric switching scenarios such as hysteretic redistribution of mobile defects, or trapping/detrapping of injected charge.

Along with many similarities, there are some drastic differences between switching behaviour of HZO and perovskite ferroelectrics. The absence of signs of coercive field increase with thickness decreasing down to sub-10nm range indicates that the switching process is very weakly influenced by the size effects. Furthermore, instead of expected increase the coercive field drops almost two times for the thickness changing from 10nm to 7 nm. As a result, a significant fraction of the 7nm capacitor area show robust and coherent switching for a bias as low as 800mV while the coercive fields extracted from piezoresponse loop array analysis are below 500mV. In this work, we proposed a hypothesis explaining the low coercive field of 7nm HZO capacitors: due to the change of opposite domain nuclei geometry the critical energy required to trigger the domain growth is significantly decreased. Obviously, the existing array of experimental data is not enough to fully validate this concept and further experimental and theoretical studies are required. In particular, accurate and statistically representative hysteresis measurements on thinner (3-5nm) capacitors would be a valuable input to complete the low-voltage switching analysis.

From the application perspective, the anomalous coercive field decrease in ultra-thin HZO shows the way towards a drastic reduction of operation voltage in CMOS-compatible ferroelectrics, where the target coercive voltage of 100-200mV looks very ambitious but still realistic. A lot of efforts need to be invested in ultrathin film processing in order to reach homogeneous low-leakage ferroelectric phase layers. However, these efforts will be fully justified by a tremendous potential of ultra-thin HZO and other HfO_2-based ferroelectric films for low-power functional electronics.

ASSOCIATED CONTENT

Supporting information: ferroelectric HZO growth and sample fabrication, technical details for off-resonance PFM measurements, additional PFM data for 30nm HZO capacitors, addressing the problem of thermal drift during the series of slow PFM scans.

ACKNOWLEDGEMENTS

The authors acknowledge the Swiss National Science Foundation for support through grant 200021_169339. T.S. acknowledges the German Research Foundation (Deutsche Forschungsgemeinschaft) for funding part of this research in the frame of the “Inferox” project (MI 1247/11-2). The authors are grateful to Prof. A. Tagantsev for very valuable and stimulating discussions.

REFERNCES

(1) Scott, J. F. Applications of Modern Ferroelectrics. *Science* **2007**, *315* (5814), 954–959.
(2) Ramesh, R. FERROELECTRICS A New Spin on Spintronics. *Nat. Mater.* **2010**, *9* (5), 380–381.

(3) Sharma, P.; Zhang, Q.; Sando, D.; Lei, C. H.; Liu, Y.; Li, J.; Nagarajan, V.; Seidel, J. Nonvolatile Ferroelectric Domain Wall Memory. *Sci. Adv.* **2017**, *3* (6), e1700512.

(4) Khan, A. I.; Chatterjee, K.; Wang, B.; Drapcho, S.; You, L.; Serrao, C.; Bakaul, S. R.; Ramesh, R.; Salahuddin, S. Negative Capacitance in a Ferroelectric Capacitor. *Nat. Mater.* **2015**, *14* (2), 182–186.

(5) Boescke, T. S.; Teichert, S.; Braeuhaus, D.; Mueller, J.; Schroeder, U.; Boettger, U.; Mikolajick, T. Phase Transitions in Ferroelectric Silicon Doped Hafnium Oxide. *Appl. Phys. Lett.* **2011**, *99* (11), 112904.

(6) Mueller, S.; Mueller, J.; Singh, A.; Riedel, S.; Sundqvist, J.; Schroeder, U.; Mikolajick, T. Incipient Ferroelectricity in Al-Doped HfO2 Thin Films. *Adv. Funct. Mater.* **2012**, *22* (11), 2412–2417.

(7) Mueller, J.; Boescke, T. S.; Schroeder, U.; Mueller, S.; Braeuhaus, D.; Boettger, U.; Frey, L.; Mikolajick, T. Ferroelectricity in Simple Binary ZrO2 and HfO2. *Nano Lett.* **2012**, *12* (8), 4318–4323.

(8) International Technology Roadmap for Semiconductors. Emerging Research Devices. Technical Report, Http://Www.Itrs2.Net/Itrs-Reports.Html, 2013.

(9) Mueller, J.; Polakowski, P.; Mueller, S.; Mikolajick, T. Ferroelectric Hafnium Oxide Based Materials and Devices: Assessment of Current Status and Future Prospects. *Ecs J. Solid State Sci. Technol.* **2015**, *4* (5), N30–N35.

(10) Yurchuk, E.; Mueller, J.; Paul, J.; Schloesser, T.; Martin, D.; Hoffmann, R.; Mueller, S.; Slesazeck, S.; Schroeeder, U.; Boschke, R.; et al. Impact of Scaling on the Performance of HfO2-Based Ferroelectric Field Effect Transistors. *Ieee Trans. Electron Devices* **2014**, *61* (11), 3699–3706.

(11) Hoffmann, M.; Schroeder, U.; Schenk, T.; Shimizu, T.; Funakubo, H.; Sakata, O.; Pohl, D.; Drescher, M.; Adelmann, C.; Materlik, R.; et al. Stabilizing the Ferroelectric Phase in Doped Hafnium Oxide. *J. Appl. Phys.* **2015**, *118* (7), 072006.

(12) Richter, C.; Schenk, T.; Park, M. H.; Tscharntke, F. A.; Grimley, E. D.; LeBeau, J. M.; Zhou, C.; Fancher, C. M.; Jones, J. L.; Mikolajick, T.; et al. Si Doped Hafnium Oxide-A “Fragile” Ferroelectric System. *Adv. Electron. Mater.* **2017**, *3* (10), 1700131.

(13) Kim, H. J.; Park, M. H.; Kim, Y. J.; Lee, Y. H.; Moon, T.; Do Kim, K.; Hyun, S. D.; Hwang, C. S. A Study on the Wake-up Effect of Ferroelectric Hf0.5Zr0.5O2 Films by Pulse-Switching Measurement. *Nanoscale* **2016**, *8* (3), 1383–1389.

(14) Park, M. H.; Lee, Y. H.; Kim, H. J.; Kim, Y. J.; Moon, T.; Do Kim, K.; Muller, J.; Kersch, A.; Schroeder, U.; Mikolajick, T.; et al. Ferroelectricity and Antiferroelectricity of Doped Thin HfO2-Based Films. *Adv. Mater.* **2015**, *27* (11), 1811–1831.

(15) Park, M. H.; Kim, H. J.; Kim, Y. J.; Lee, Y. H.; Moon, T.; Do Kim, K.; Hyun, S. D.; Hwang, C. S. Study on the Size Effect in Hf0.5Zr0.5O2 Films Thinner than 8 Nm before and after Wake-up Field Cycling. *Appl. Phys. Lett.* **2015**, *107* (19), 192907.

(16) Chernikova, A.; Kozodaev, M.; Markeev, A.; Negrov, D.; Spiridonov, M.; Zarubin, S.; Bak, O.; Buraohain, P.; Lu, H.; Suvorova, E.; et al. Ultrathin Hf0.5Zr0.5O2 Ferroelectric Films on Si. *Acs Appl. Mater. Interfaces* **2016**, *8* (11), 7232–7237.

(17) Sang, X.; Grimley, E. D.; Schenk, T.; Schroeder, U.; LeBeau, J. M. On the Structural Origins of Ferroelectricity in HfO2 Thin Films. *Appl. Phys. Lett.* **2015**, *106* (16), 162905.

(18) Materlik, R.; Kuenneth, C.; Kersch, A. The Origin of Ferroelectricity in Hf1-XZrxO2: A Computational Investigation and a Surface Energy Model. *J. Appl. Phys.* **2015**, *117* (13), 134109.

(19) Grimley, E. D.; Schenk, T.; Mikolajick, T.; Schroeder, U.; LeBeau, J. M. Atomic Structure of Domain and Interphase Boundaries in Ferroelectric HfO2. *Adv. Mater. Interfaces* **2018**.

(20) Fengler, F. P. G.; Nigon, R.; Muralt, P.; Grimley, E. D.; Sang, X.; Sessi, V.; Hentschel, R.; LeBeau, J. M.; Mikolajick, T.; Schroeder, U. Analysis of Performance Instabilities of Hafnia-Based Ferroelectrics Using Modulus Spectroscopy and Thermally Stimulated Depolarization Currents. *Adv. Electron. Mater.* **2018**, *4* (3), 1700547.

(21) Martin, D.; Muller, J.; Schenk, T.; Arruda, T. M.; Kumar, A.; Strelcov, E.; Yurchuk, E.; Muller, S.; Pohl, D.; Schroder, U.; et al. Ferroelectricity in Si-Doped HfO2 Revealed: A Binary Lead-Free Ferroelectric. *Adv. Mater.* **2014**, *26* (48), 8198–8202.

(22) Balke, N.; Maksymovych, P.; Jesse, S.; Herklotz, A.; Tselev, A.; Eom, C. B.; Kravchenko, I. I.; Yu, P.; Kalinin, S. V. Differentiating Ferroelectric and Nonferroelectric Electromechanical Effects with Scanning Probe Microscopy. *Acs Nano* **2015**, *9* (6), 6484–6492.

(23) Vasudevan, R. K.; Balke, N.; Maksymovych, P.; Jesse, S.; Kalinin, S. V. Ferroelectric or Non-Ferroelectric: Why so Many Materials Exhibit "Ferroelectricity" on the Nanoscale. *Appl. Phys. Rev.* **2017**, *4* (2), 021302.

(24) Vasudevan, R. K.; Marincel, D.; Jesse, S.; Kim, Y.; Kumar, A.; Kalinin, S. V.; Trolier-McKinstry, S. Polarization Dynamics in Ferroelectric Capacitors: Local Perspective on Emergent Collective Behavior and Memory Effects. *Adv. Funct. Mater.* **2013**, *23* (20), 2490–2508.

(25) Setter, N.; Damjanovic, D.; Eng, L.; Fox, G.; Gevorgian, S.; Hong, S.; Kingon, A.; Kohlstedt, H.; Park, N. Y.; Stephenson, G. B.; et al. Ferroelectric Thin Films: Review of Materials, Properties, and Applications. *J. Appl. Phys.* **2006**, *100* (5), 051606.

(26) Chouprik, A.; Zakharchenko, S.; Spiridonov, M.; Zarubin, S.; Chernikova, A.; Kirtaev, R.; Buragohain, P.; Gruverman, A.; Zenkevich, A.; Negrov, D. Ferroelectricity in Hf0.5Zr0.5O2 Thin Films: A Microscopic Study of the Polarization Switching Phenomenon and Field-Induced Phase Transformations. *Acs Appl. Mater. Interfaces* **2018**, *10* (10), 8818–8826.

(27) Starschich, S.; Griesche, D.; Schneller, T.; Waser, R.; Boettger, U. Chemical Solution Deposition of Ferroelectric Yttrium-Doped Hafnium Oxide Films on Platinum Electrodes. *Appl. Phys. Lett.* **2014**, *104* (20), 202903.

(28) Starschich, S.; Schenk, T.; Schroeder, U.; Boettger, U. Ferroelectric and Piezoelectric Properties of Hf(1-x)ZrxO(2) and Pure ZrO2 Films. *Appl. Phys. Lett.* **2017**, *110* (18), 182905.

(29) Mittmann, T.; Fengler, F. P. G.; Richter, C.; Park, M. H.; Mikolajick, T.; Schroeder, U. Optimizing Process Conditions for Improved Hf-1 - ZrxO2 Ferroelectric Capacitor Performance. *Microelectron. Eng.* **2017**, *178*, 48–51.

(30) Park, M. H.; Kim, H. J.; Kim, Y. J.; Lee, W.; Moon, T.; Hwang, C. S. Evolution of Phases and Ferroelectric Properties of Thin Hf0.5Zr0.5O2 Films According to the Thickness and Annealing Temperature. *Appl. Phys. Lett.* **2013**, *102* (24), 242905.

(31) Rodriguez, B. J.; Callahan, C.; Kalinin, S. V.; Proksch, R. Dual-Frequency Resonance-Tracking Atomic Force Microscopy. *Nanotechnology* **2007**, *18* (47), 475504.

(32) Jesse, S.; Kalinin, S. V.; Proksch, R.; Baddorf, A. P.; Rodriguez, B. J. The Band Excitation Method in Scanning Probe Microscopy for Rapid Mapping of Energy Dissipation on the Nanoscale. *Nanotechnology* **2007**, *18* (43), 435503.

(33) Chen, L.; Nagarajan, V.; Ramesh, R.; Roytburd, A. L. Nonlinear Electric Field Dependence of Piezoresponse in Epitaxial Ferroelectric Lead Zirconate Titanate Thin Films. *J. Appl. Phys.* **2003**, *94* (8), 5147–5152.

(34) Mulaosmanovic, H.; Ocker, J.; Mueller, S.; Schroeder, U.; Mueller, J.; Polakowski, P.; Flachowsky, S.; van Bentum, R.; Mikolajick, T.; Slesazeck, S. Switching Kinetics in Nanoscale Hafnium Oxide Based Ferroelectric Field-Effect Transistors. *Acs Appl. Mater. Interfaces* **2017**, *9* (4), 3792–3798.

(35) Park, M. H.; Lee, Y. H.; Kim, H. J.; Schenk, T.; Lee, W.; Do Kim, K.; Fengler, F. P. G.; Mikolajick, T.; Schroeder, U.; Hwang, C. S. Surface and Grain Boundary Energy as the Key Enabler of Ferroelectricity in Nanoscale Hafnia-Zirconia: A Comparison of Model and Experiment. *Nanoscale* **2017**, *9* (28), 9973–9986.

(36) Gerra, G.; Tagantsev, A. K.; Setter, N. Surface-Stimulated Nucleation of Reverse Domains in Ferroelectrics. *Phys. Rev. Lett.* **2005**, *94* (10), 107602.

(37) Xu, R.; Gao, R.; Reyes-Lillo, S. E.; Saremi, S.; Dong, Y.; Lu, H.; Chen, Z.; Lu, X.; Qi, Y.; Hsu, S.-L.; et al. Reducing Coercive-Field Scaling in Ferroelectric Thin Films via Orientation Control. *ACS Nano* **2018**.

(38) Kay, H.; Dunn, J. Thickness Dependence of Nucleation Field of Triglycine Sulphate. *Philos. Mag.* **1962**, *7* (84), 2027-.

(39) Tagantsev, A.; Landivar, M.; Colla, E.; Setter, N. Identification of Passive Layer in Ferroelectric Thin-Films from Their Switching Parameters. *J. Appl. Phys.* **1995**, *78* (4), 2623–2630.

(40) Dawber, M.; Chandra, P.; Littlewood, P. B.; Scott, J. F. Depolarization Corrections to the Coercive Field in Thin-Film Ferroelectrics. *J. Phys.-Condens. Matter* **2003**, *15* (24), L393–L398.

(41) Landauer, R. Electrostatic Considerations in $BaTiO_3$ Domain Formation during Polarization Reversal. *J. Appl. Phys.* **1957**, *28* (2), 227–234.

(42) Tagantsev, A.; Cross, E.; Fousek, J. *Domains in Ferroic Crystals and Thin Films*; Springer: New York, 2010.

Table of Contents/Abstract Graphic

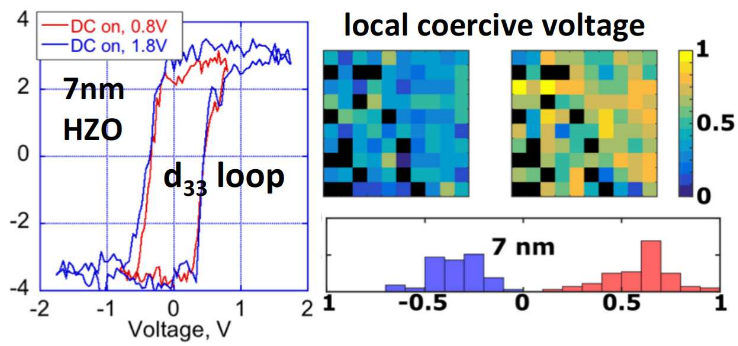

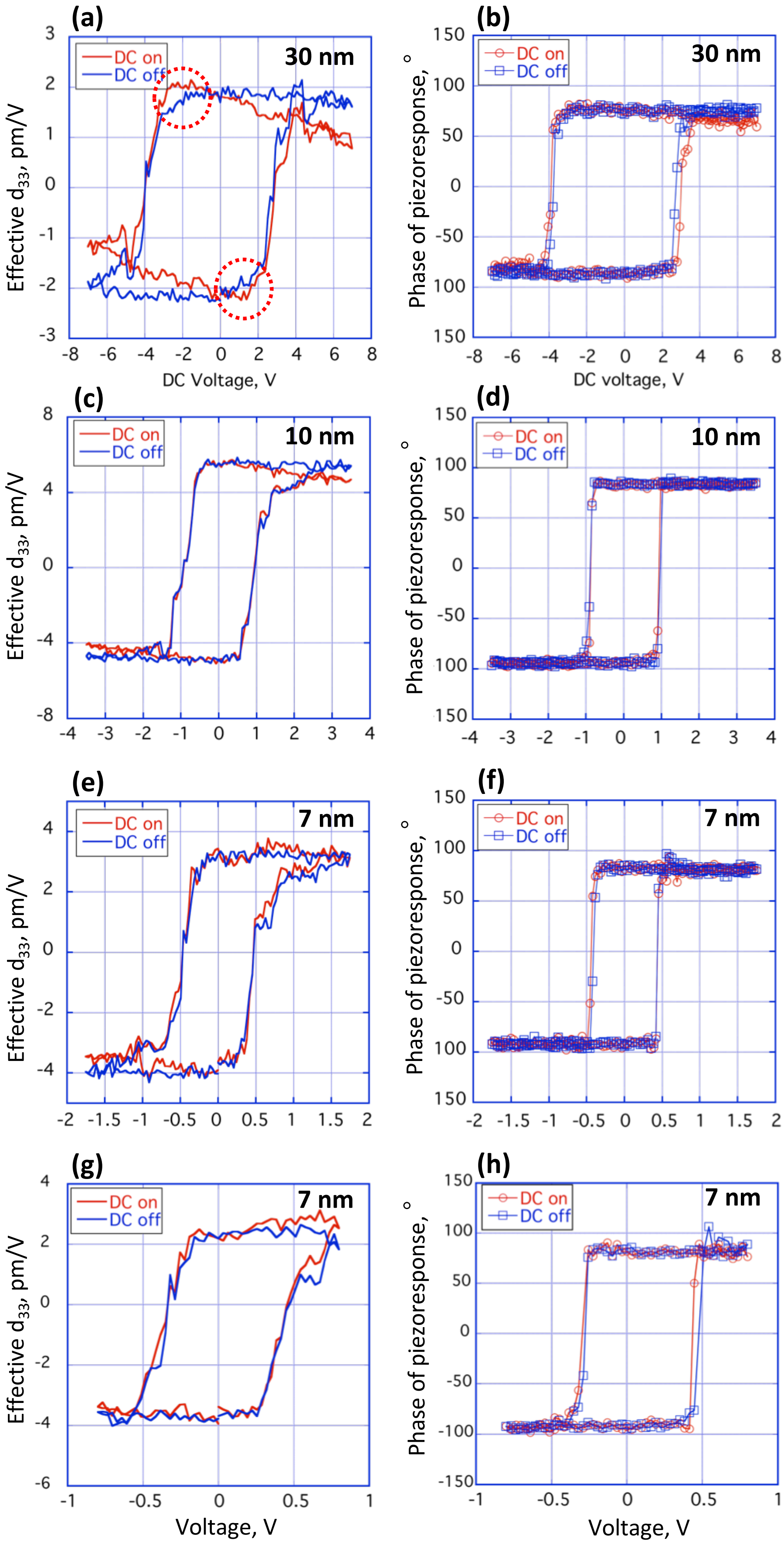

Figure 1. Loops of effective d_{33} and phase of local piezoresponse of HZO capacitors with thickness of 30nm **(a, b)**, 10nm **(c, d)**, and 7nm **(e, f)**. **g, h** Effective d_{33} **(g)** and phase **(h)** of local piezoresponse for the 7nm HZO capacitor measured with switching voltage amplitude of 800mV. All loops were measured in the off-resonance mode through the top electrode.

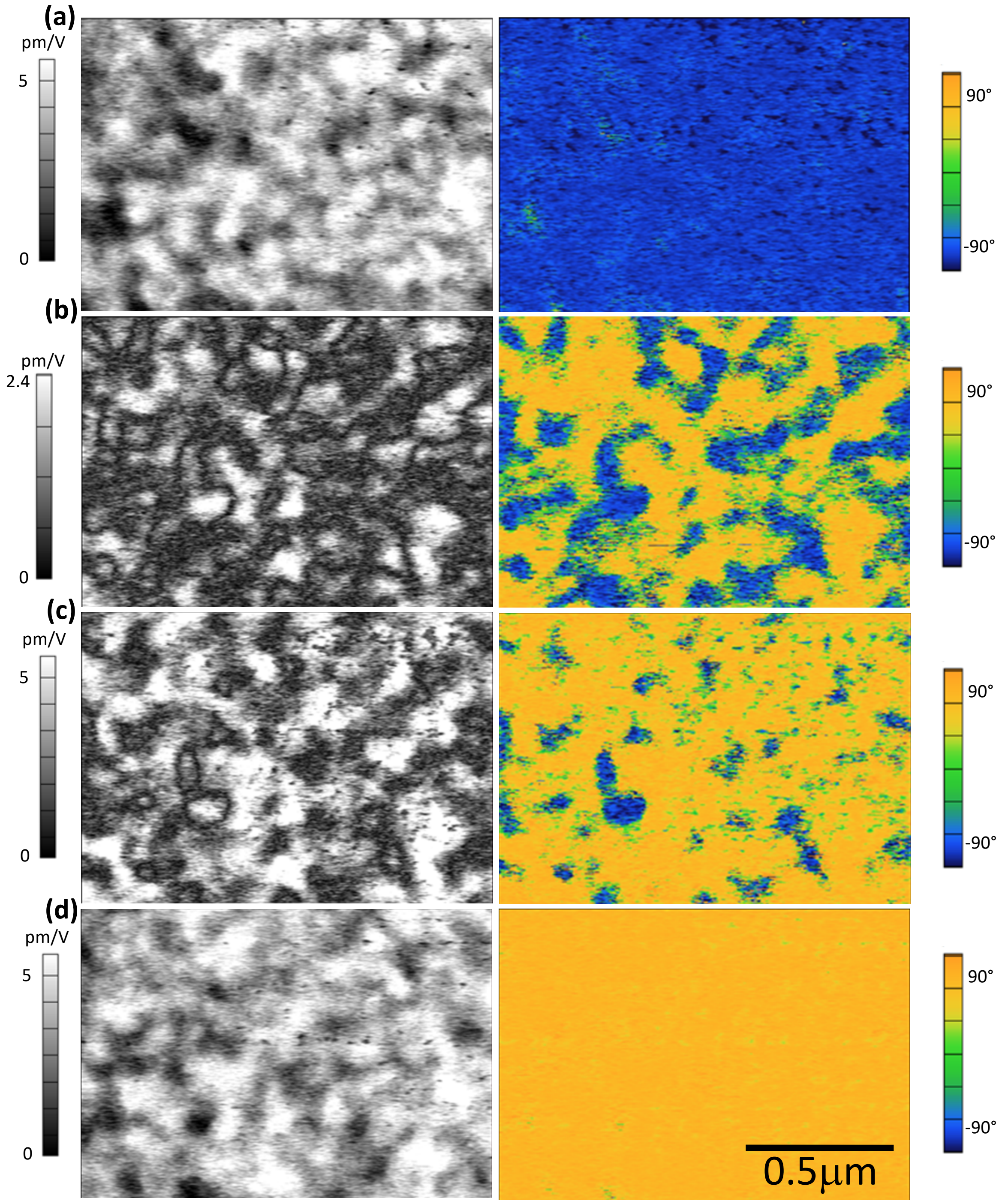

Figure 2. 1x1.4μm^2 scans of amplitude (left) and phase (right) of local piezoelectric response measured on the 10nm HZO capacitor in the off-resonance mode. The sequential images **a-d** represent the stages of polarization reversal. The capacitor is poled with the top electrode bias of -3V **(a)**, then the polarization was partially reversed with +1.3V **(b)** and with +1.7V **(c)**. Finally the capacitor was poled with the top electrode bias of +3V **(d).**

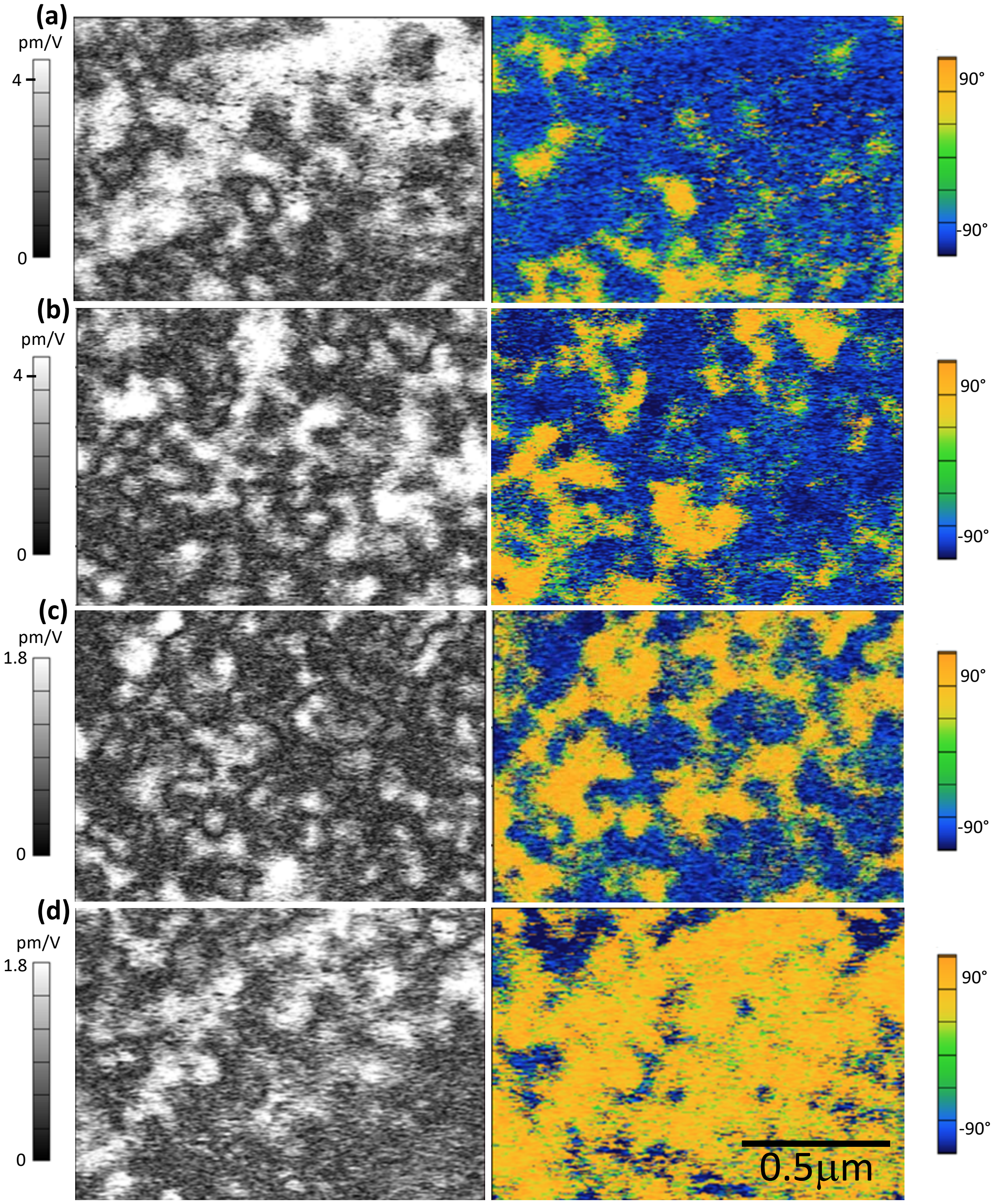

Figure 3. 1x1.4μm^2 scans of amplitude (left) and phase (right) of local piezoelectric response measured on the 7nm HZO capacitor in the off-resonance mode. The sequential images **a-d** represent the stages of polarization reversal. The capacitor is poled with the top electrode bias of -1.8V **(a)**, then the polarization was partially reversed with +0.7V **(b)** and with +0.9V **(c)**. Finally the capacitor was poled with the top electrode bias of +1.8V **(d).**

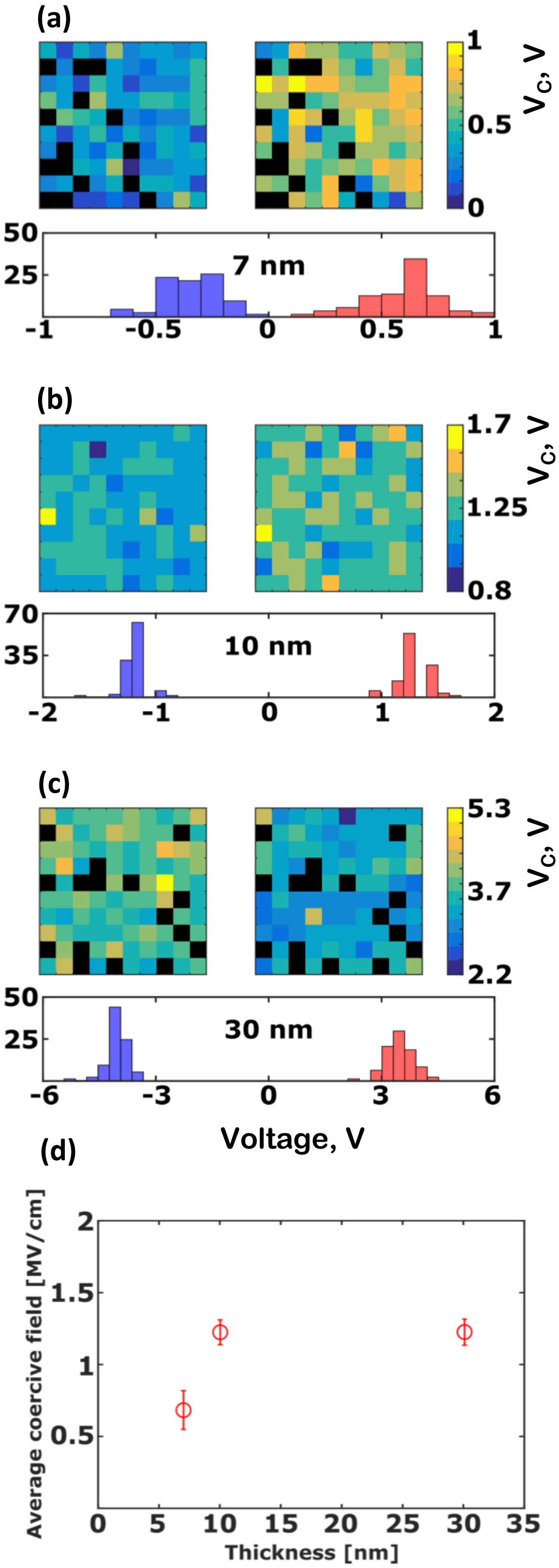

Figure 4. **a-c**, 1x1μm^2 maps of negative (left) and positive (right) coercive voltages (V_C) extracted from the local piezoresponse loops measured through the top electrode on the HZO capacitors with thickness of 7nm **(a)**, 10nm **(b)** and 30nm **(c)**. The black squares represent the areas where the piezoresponse could not be measured or switched. **d**, Thickness dependence of average coercive fields calculated from the maps **a-c**.

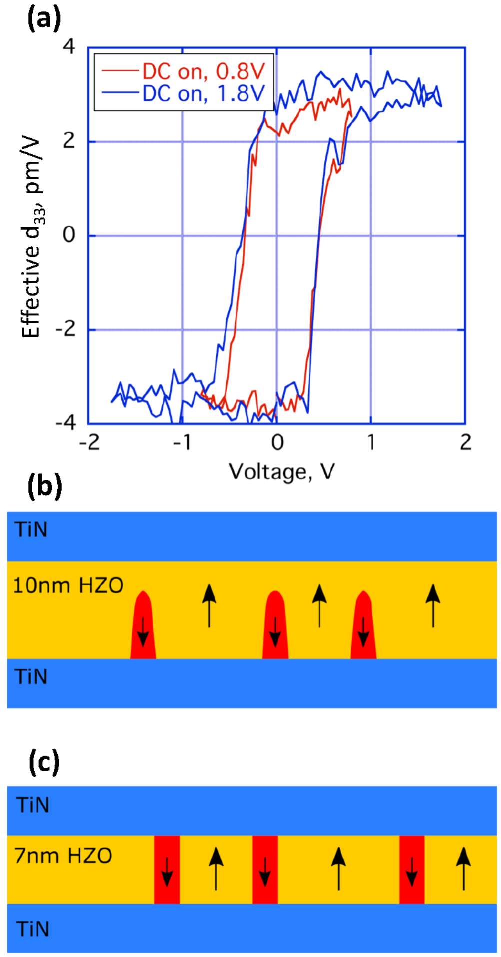

Figure 5. **a**, Comparison of the effective d_{33} loops measured on the 7nm HZO capacitor with switching voltage amplitude of 0.8V and 1.8V. The two loops measured on the same spot show same V_c and very close d_{33} values at V=0. **b, c,** Two different modes of opposite domain nucleation. **b,** standard nucleation model, where the nuclei need to overcome the electrostatic energy associated with depolarizing effect. **c,** scenario proposed for ultra-thin films (7nm), where the cylindrical nuclei extend from the bottom to top interface. Such nuclei are not influenced by depolarizing field and their growth requires a lower critical energy compared to the case **(b)**.